
Limitations on Space-based Air Fluorescence Detector Apertures obtained from IR Cloud Measurements

John Krizmanic,^{1,2} Pierre Sokolsky³, and Robert Streitmatter²

(1) *Universities Space Research Association*

(2) *NASA Goddard Space Flight Center, Greenbelt, Maryland 20771, USA*

(3) *High Energy Astrophysics Institute, University of Utah, Salt Lake City, Utah 84112, USA*

Abstract

The presence of clouds between an airshower and a space-based detector can dramatically alter the measured signal characteristics due to absorption and scattering of the photonic signals. Furthermore, knowledge of the cloud cover in the observed atmosphere is needed to determine the instantaneous aperture of such a detector. Before exploring the complex nature of cloud-airshower interactions, we examine a simpler issue. We investigate the fraction of ultra-high energy cosmic ray events that may be expected to occur in volumes of the viewed atmosphere non-obscured by clouds. To this end, we use space-based IR data in concert with Monte Carlo simulated 10^{20} eV airshowers to determine the acceptable event fractions. Earth-observing instruments, such as MODIS, measure detailed cloud configurations via a CO₂-slicing technique that can be used to determine cloud-top altitudes over large areas. Thus, events can be accepted if their observed 3-dimensional endpoints occur above low clouds as well as from areas of cloud-free atmosphere. An initial analysis has determined that by accepting airshowers that occur above low clouds, the non-obscured acceptance can be increased by approximately a factor of 3 over that obtained using a cloud-free criterion.

1. Introduction

Using the air fluorescence technique, the space-based experiments EUSO [1] and OWL [4] will image the UV nitrogen fluorescence signal from extended airshowers with a spatial resolution of ~ 1 km² (on the ground) while instantaneously monitoring areas approaching 10^6 km². The effects of clouds must be well understood as clouds can obscure or modify the signal strengths and profiles of the airshowers. The incorporation of a LIDAR system has been proposed to be used in conjunction with the EUSO and OWL detectors, but the scanning requirements imposed by the nearly mega-pixel count and the rapidly moving

footprint(s) lead to severe operational requirements. An alternate approach to determine the cloud properties is the use of meteorological measurements. The MODIS instruments [3] on the Terra and Aqua satellites provide derived cloud property measurements from IR measurements with a spatial resolution of ~ 1 km² on the ground. Using the technique of CO₂ slicing [7], cloud-top altitudes can be determined and lead to 3-dimensional cloud profiles. The availability of these and future meteorological measurements could be used by space-based air fluorescence experiments to define clear apertures and relax LIDAR operational constraints.

In a previous paper [5], we used simulated airshowers superimposed over MODIS measured scenes and obtained *the fraction of tracks that occur in cloud-free portions of the atmosphere*. This analysis used a cloud-mask product that provides a probabilistic determination of whether a particular 1 km² pixel contains a cloud. Using a conservative selection criteria defined by requiring no cloudy pixels within 3 km of the observed portion of a simulated airshower, we determined that the mean of the distribution was 6.5%. Assuming a 15% duty cycle imposed by moonless night along with other operational constraints, a 6.5% clear fraction leads to a disconcerting 1% effective duty cycle.

In this paper, we present the first results on the potential of recovering airshowers with observed endpoints that occur above low clouds and thus are unobscured. This is accomplished by employing another MODIS data product which yields cloud-top pressures, i.e. cloud-top altitudes, but on a courser 5×5 km² pixel scale. The unobscured event fraction is then determined by combining the cloud-free fraction with the low-cloud fraction.

2. Method of Analysis

A simulated, airshower event sample was generated using the OWL Monte Carlo [2] assuming an isotropic flux of 10^{20} eV protons. The two OWL instruments [6] were configured to be in 1000 km orbits with a 500 km satellite separation. The 3-dimensional airshower tracks were reconstructed using the stereo reconstruction technique with the track endpoints determined by requiring observation by both instruments. The approximately 1700 tracks were then superimposed upon 78 different MODIS scenes defined by the MODIS Collection4 cloud-top product. Each pixel was coded with either being clear, having a cloud top with an altitude of 3 km or less, or a cloud top with an altitude higher than 3 km. The spatial location of the xy-projected track lengths were then compared to the MODIS cloud pixel information to determine whether the tracks occurred in a clear, low-cloud, or high-cloud portion of the MODIS scene. The extended nature of the airshowers will lead to a reduced acceptance as compared to that expected by determining the cloud-free or low-cloud pixel fractions.

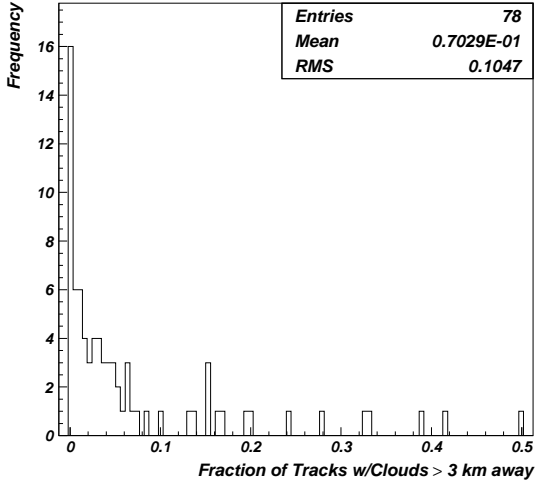


Fig. 1. Distribution of fractional clear aperture obtained from the 1 km^2 MODIS cloud-mask data.

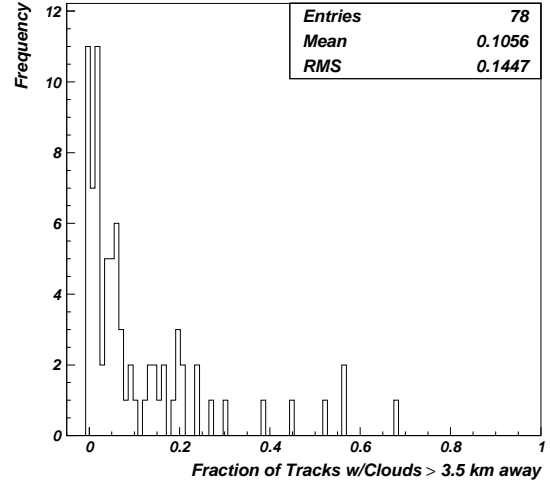


Fig. 2. Distribution of fractional clear aperture obtained from the $5 \times 5 \text{ km}^2$ MODIS cloud-top pressure data.

3. Results

Figure 1 shows the distribution of the cloud-free track fraction using the 1 km^2 cloud-mask product for the 78 MODIS scenes located near the equator used in this study. The analysis follows that employed in our previous paper [5]: a track is considered in a cloud-free portion of the atmosphere if no cloudy pixels are within 3 km of the observed track. The results presented in Figure 1 employed a newer version, Collection4, of the cloud-mask determining algorithm. The mean of 7% matches well to the 6.5% we had obtained for a slightly larger MODIS data set by using a previous version of the MODIS cloud-mask algorithm. The 78 scenes used in this study are a subset of the 85 scenes

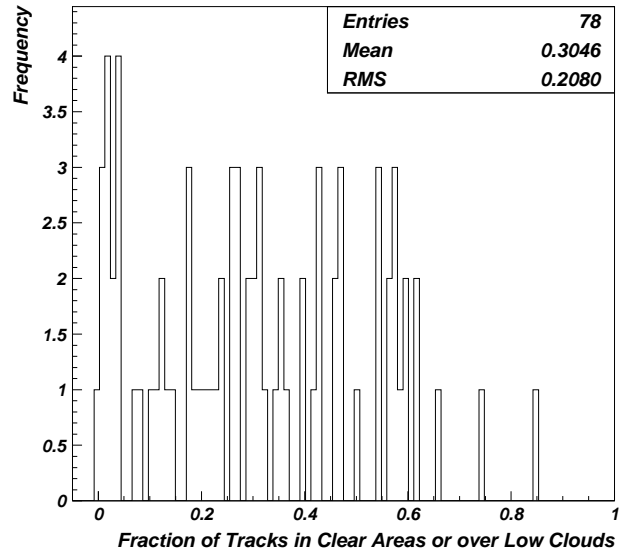


Fig. 3. Distribution of fractional clear and low-cloud aperture obtained from the $5 \times 5 \text{ km}^2$ MODIS cloud-top pressure data.

used in the original study. Figure 2 shows the distribution of cloud-free track fractions for the 78 MODIS scenes using the MODIS cloud-top data product. The cloud-free fractions were determined by requiring no cloudy pixels to be within 3.5 km of the track. The slightly larger value of 3.5 km is imposed by the courser 5×5 km² pixel size used in the cloud-top product. Note that the cloud-free fraction of 10.7% obtained by this analysis is in relatively good agreement with the 7% obtained from the 1 km² cloud-mask analysis.

Figure 3 shows the distribution of the fraction of tracks that occur over either cloud-free areas or have a portion of the xy-projected track over clouds with cloud-top heights of less than 3 km. A track over low clouds was accepted if it was at least 3.5 km from a pixel with a > 3 km altitude cloud and has an observed track endpoint at an altitude 4 km or higher. The simulated event sample has 53% of the tracks with observed endpoints above 4 km in altitude. The distribution in Figure 3 exhibits a mean of over 30% and is flatter than that for the cloud-free fraction (Figure 2). The 30% value is a factor of 3 larger than that for the cloud-free fraction. If the track endpoint requirement is increased to 5 km for low-cloud acceptance, the mean of the combined cloud-free and low-cloud distribution is reduced to 26%.

4. Discussion

The ability to determine the altitudes of airshowers and cloud tops allows for a significant increase in the acceptance of events by including tracks whose observable endpoints occur above low clouds. The potential for the increase is echoed in the 16% cloud-free versus 53% cloud-free+low-cloud pixel fractions obtained from the MODIS cloud-top data used in this study.

We would like to thank Bill Ridgway for invaluable discussions and for the generation of the MODIS data files.

5. References

1. <http://www.euso-mission.org/>
2. Krizmanic, J. for the OWL Collaboration 2001, Proc. 27th ICRC, Vol. 2, 861
3. <http://modis-atmos.gsfc.nasa.gov/>
4. <http://owl.gsfc.nasa.gov/>
5. Sokolsky P., Krizmanic J. 2003, astro-ph/0302501, submitted to Astroparticle Physics
6. Streitmatter R. et al. 2002, <http://owl.gsfc.nasa.gov/WP10c.PDF>
7. Stumpf R., Pennock J. 1989, Jour. Geophys. Res. 94(C10), 14,363